Korean J. Chem. Eng., 34(10), 2610-2618 (2017)
DOI: 10.1007/s11814-017-0164-4

pISSN: 0256-1115
eISSN: 1975-7220

Reductive amination of ethanol to ethylamines over Ni/Al_2O_3 catalysts

Jung-Hyun Park*,‡, Eunpyo Hong,‡, Sang Hee An**, Dong-Hee Lim***, and Chae-Ho Shin**,†**

*Greenhouse Gas Resources Research Group, Korea Research Institute of Chemical Technology, Daejeon 34114, Korea
**Department of Chemical Engineering, Chungbuk National University, Chungbuk 28644, Korea
***Department of Environmental Engineering, Chungbuk National University, Chungbuk 28644, Korea
(*Received 12 April 2017 • accepted 12 June 2017*)

Abstract−$Ni(x)/Al_2O_3$ (x=wt%) catalysts with Ni loadings of 5-25 wt% were prepared via a wet impregnation method on an γ-Al_2O_3 support and subsequently applied in the reductive amination of ethanol to ethylamines. Among the various catalysts prepared, $Ni(10)/Al_2O_3$ exhibited the highest metal dispersion and the smallest Ni particle size, resulting in the highest catalytic performance. To reveal the effects of reaction parameters, a reductive amination process was performed by varying the reaction temperature (T), weight hourly space velocity (WHSV), and NH_3 and H_2 partial pressures in the reactions. In addition, on/off experiments for NH_3 and H_2 were also carried out. In the absence of NH_3 in the reactant stream, the ethanol conversion and selectivities towards the different ethylamine products were significantly reduced, while the selectivity to ethylene was dominant due to the dehydration of ethanol. In contrast, in the absence of H_2, the selectivity to acetonitrile significantly increased due to dehydrogenation of the imine intermediate. Although a small amount of catalyst deactivation was observed in the conversion of ethanol up to 10 h on stream due to the formation of nickel nitride, the $Ni(10)/Al_2O_3$ catalyst exhibited stable catalytic performance over 90 h under the optimized reaction conditions (i.e., T=190 °C, WHSV=0.9 h^{-1}, and $EtOH/NH_3/H_2$ molar ratio=1/1/6).

Keywords: Ni/Al_2O_3 Catalyst, Ethanol, Reductive Amination, Ethylamines, Nickel Nitride

INTRODUCTION

Ethylamines (EAs) have been widely used as intermediates to produce fine chemicals, such as herbicides, pharmaceuticals, textile chemicals, rubbers, and corrosion inhibitors [1-3]. Due to the increasing demand for amine-containing compounds in the chemical industry, a variety of methods for their syntheses have been proposed, including the hydrogenation of nitrile compounds [4,5], the reductive amination of ethanol (EtOH) and acetaldehyde [1-3,6], and the hydroamination of olefins [7]. Among the various approaches, reductive amination has been considered a promising route for the preparation of EAs due to the environmentally friendly nature of the process [3,8]. In addition, the synthesis of EAs via other reaction pathways usually requires harsh reaction conditions, including high temperatures and pressures, while the amination reaction can instead proceed under relatively mild conditions [1].

As shown in Fig. 1, the reductive amination of EtOH progresses through successive stages, beginning with the dehydrogenation of EtOH to acetaldehyde [9-12]. An imine intermediate is then obtained by condensation and reaction of the carbonyl compound with NH_3. As amine compounds can be produced as either primary, secondary, or tertiary amines, monoethylamine (MEA) can be synthesized via the hydrogenation of the imine intermediate, while diethylamine (DEA) and triethylamine (TEA) are formed by consecutive reactions with EtOH. As hydrogenation/dehydrogenation processes are involved in the preparation of EAs via this mechanism, a catalyst surface bearing metallic functionalities must be employed. In this context, the dispersion and reducibility of the metal species are key factors to determine catalytic performances in the reductive amination reaction [1,9,13,14].

The noble metal catalysts containing Pt, Pd, and Rh have been applied in reductive amination reactions due to their excellent hydrogenation and dehydrogenation capabilities [15-18]. However, their application has been restricted due to high costs, and thus the development of alternative catalysts has received growing attention. From this perspective, Ni- and Co-containing catalysts have been widely studied for application in reductive amination reactions because of their suitable activities and selectivities, in addition to their wide availability [1,2,9,11-13,19]. Sewell et al. [2] investigated the reductive amination of alcohols over Ni- or Co-catalysts supported on SiO_2. Although a higher EtOH conversion was obtained for the Co-based catalyst compared to that of the Ni-based catalyst, selectivity towards the formation of different amine species varied depending on the type of metal. More specifically, the Co-based catalyst favored the production of the primary amine, while the Ni-based catalyst was more selective towards the secondary amine. In addition, the deactivation of these catalysts by the formation of metal nitrides through interactions between NH_3 and the active metal species has also been well documented [13,20,21].

We herein report the preparation of Ni/Al_2O_3 catalysts containing different Ni loadings for application in the reductive amination of EtOH to EAs. In addition, the relationship between the metallic surface area and the Ni loading was examined, and the catalytic

†To whom correspondence should be addressed.
E-mail: chshin@chungbuk.ac.kr
‡These authors contributed equally to this work.

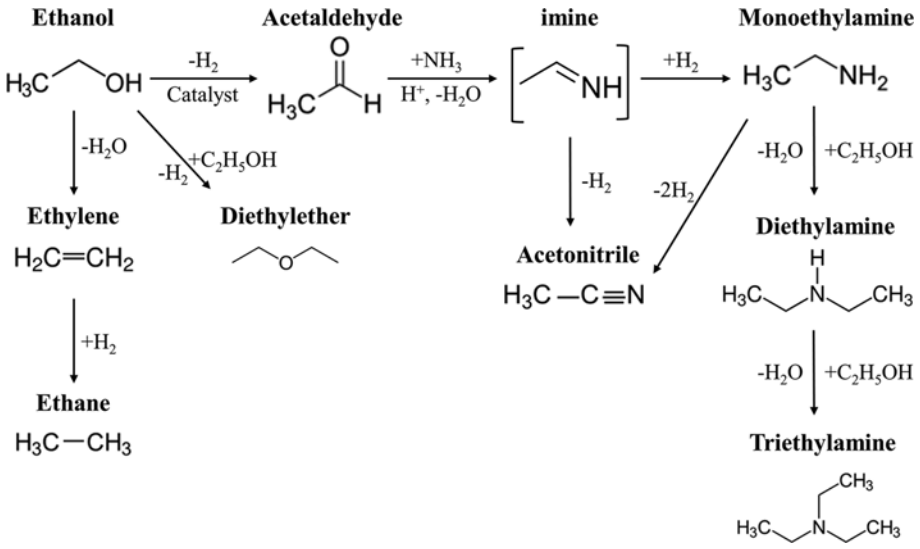

Fig. 1. Possible reaction pathways for the reductive amination of ethanol.

performance of the different catalysts were carefully investigated. As reaction parameters have been shown to significantly influence alcohol conversion and selectivity towards different nitrogen-containing compounds [1,2,9], we also examined the influence of reaction temperature (T), weight hourly space velocity (WHSV), and the partial pressures of NH_3 and H_2. Finally, to further understand the effects of the key reactants, on/off experiments for NH_3 and H_2 were also carried out.

EXPERIMENTAL

1. Catalyst Preparation

Ni/Al_2O_3 catalysts with Ni loading ranging from 5 to 25 wt% were prepared via a wet impregnation method with a nickel nitrate hexahydrate solution ($Ni(NO_3)_2{\cdot}6H_2O$, >98%, Samchun) and commercial γ-Al_2O_3 (S_{BET}=194 m^2/g, particle size=100-180 μm, Procatalyse) as the Ni metal precursor and the support, respectively. The precursor and the support in the desired ratio was stirred at room temperature for 1 h, prior to evaporation of the solvent at 70 °C using a rotary evaporator (Eylar N1000). The impregnated sample was then dried at 100 °C for 12 h, and subsequently calcined at 500 °C for 2 h under a flow of air. The prepared Ni/Al_2O_3 catalysts were denoted as $Ni(x)/Al_2O_3$, where x (x=5, 10, 15, 20, and 25) represents the Ni loading in weight percent (wt%).

2. Characterization

X-ray diffraction (XRD) patterns were obtained using a Rigaku diffractometer (Ultima IV) equipped with a Cu-Kα X-ray source operating at 40 kV and 40 mA. The crystalline phases were identified by matching the patterns to the JCPDS powder diffraction files, and the particle sizes of NiO and Ni were calculated using the Scherrer equation. The specific surface area, total pore volume, and average pore size of the $Ni(x)/Al_2O_3$ catalysts were then determined by N_2-sorption isotherms at −196 °C on a Micromeritics ASAP2020 apparatus. Prior to N_2-sorption analysis, the samples were degassed at 250 °C for 4 h. The specific surface areas of the samples were then calculated using the Brunauer-Emmet-Teller (BET) equation in the relative pressure range between 0.05-0.2. The total pore volumes were obtained from the volumes of N_2 adsorbed at P/P_0= 0.995, and the average pore sizes were calculated from the desorption branch using the Barrett-Joyner-Hallenda (BJH) equation.

The metal dispersions, particle sizes, and metallic surface areas of the different $Ni(x)/Al_2O_3$ catalysts were determined by H_2 chemisorption (Micromeritics ASAP2020C). Prior to analysis, the samples (0.3 g) were reduced at 600 °C for 3 h under a flow of H_2. Each sample was then cooled to 100 °C under reduced pressure, and the chemisorption isotherm was obtained from the difference between the first and second adsorption isotherms. The first isotherm involved both quantities of chemisorption and physisorption, while second contained only the physisorbed quantity. In addition, the metal dispersion was calculated for each sample assuming an H/Ni stoichiometry of 1.0, while the reduction degree of each $Ni(x)/Al_2O_3$ catalyst was determined using the O_2 titration method. The O_2 titration method was subsequently conducted on an identical apparatus, following the H_2 chemisorption. The sample used in the H_2 chemisorption experiment was evacuated at 300 °C for 1 h, and the reduction degree was calculated in combination with the following equation: [the amount of O_2 consumption (mmol O_2; $2Ni+O_2 \rightarrow 2NiO$)/[the theoretical amount of H_2 consumption with the assumption of fully reduced nickel oxides (mmol H_2; $NiO+H_2 \rightarrow Ni^0+H_2O$)]×100)] [22], where the amount of O_2 consumption was determined at 300 °C by plotting the amount of consumed O_2 as a function of the O_2 partial pressure, and back extrapolating to zero.

H_2-temperature programmed reduction (H_2-TPR) was performed using a quadrupole mass spectrometer (QMS, Balzers QMS 200) as the detector. Each sample (0.1 g) was loaded in a quartz reactor (I.D. 12 mm) and pretreated at 400 °C for 1 h under a flow of Ar (50 cm^3/min). After cooling to 50 °C, a flow of 5% H_2/Ar (50 cm^3/min) was then introduced into the catalyst bed, and the temperature was increased to 800 °C with a heating rate of 10 °C/min. The mass signal of H_2 (m/z=2) was collected by QMS. To determine the surface chemical state of the catalyst both before and after the

reaction, X-ray photoelectron spectroscopy (XPS) was performed on PHI Quantera II (Ulvac-PHI) with Al-Kα radiation and hν= 1,486.6 eV. The binding energy was corrected based on adventitious carbon, C1s, at 284.6 eV.

3. Reductive Amination of Ethanol over the Prepared Ni/Al_2O_3 Catalysts

The reductive amination of EtOH was performed in a fixed-bed reactor under atmospheric pressure. Prior to the reaction, the catalysts were reduced at 600 °C for 3 h under a flow of H_2 (50 cm^3/min). The standard reaction conditions were as follows: 0.2 g catalyst, T=190 °C, WHSV=0.9 h^{-1}, total flow rate=50 cm^3/min, a molar feed composition of EtOH/NH_3/H_2=1/3/6 (with N_2 balance), and a fixed EtOH partial pressure of 3 kPa. To investigate the effect of the different reaction parameters on the reductive amination of EtOH, variations in the reaction temperature (170-210 °C), WHSV (0.55-2.38 h^{-1}), total flow rate (30-160 cm^3/min), NH_3 partial pressure (1.5-9 kPa), and H_2 partial pressure (0-24 kPa) were examined. The reaction products were analyzed using a gas chromatograph (CP9001, Chrompack) equipped with a CP-Volamine capillary column (60×0.32 mm) and a flame ionization detector (FID). The conversion of EtOH, the product selectivity, and the WHSV were defined as follows:

$$\text{Conversion (X, \%)} = \frac{F_{EtOH}\ \text{reacted}}{F_{EtOH}\ \text{fed}} \times 100\%$$

$$\text{i Component selectivity (S, \%)} = \frac{F_i C_i}{\Sigma F_i C_i} \times 100\%$$

$$\text{WHSV } (h^{-1}) = \frac{F_{EtOH}\ (\text{mol/h}) \times MW_{EtOH}\ (\text{g/mol})}{\text{Quantity of catalyst (g)}}$$

where F_{EtOH} and F_i are molar flow rates of EtOH and the product (i, i.e., EAs, acetonitrile, and ethylene), respectively, MW_{EtOH} is the molecular weight of EtOH, and C_i is the number of carbon atoms in the product i.

RESULTS AND DISCUSSION

1. Characterization

Following preparation of the calcined and reduced Ni(x)/Al_2O_3 catalysts, their structures were initially examined by XRD, as shown in Fig. 1. As expected, NiO (JCPDS No. 47-1049) and γ-Al_2O_3 (JCPDS No. 29-0063) phases were observed in the diffraction patterns of the calcined Ni(x)/Al_2O_3 catalysts (Fig. 2(a)), while metallic Ni (JCPDS No. 04-0850) and the γ-Al_2O_3 phase were detected following the reduction process (Fig. 2(b)). However, due to high dispersion of the Ni species on the γ-Al_2O_3 support, NiO (calcined samples) and Ni (reduced samples) phases were not observed below a Ni loading of 10 wt%. Particle sizes of NiO (2θ=43.4°) and Ni (2θ=44.5°) calculated using the Scherrer equation are presented in Table 1. Upon increasing the Ni loading, the particle sizes of NiO and Ni increased due to sintering of the particles, which resulted in the formation of agglomerated bulk NiO species. More specifically, for the NiO particles in the Ni(x)/Al_2O_3 catalysts, an increase in size from 14.2 (x=15) to 17.6 nm (x=25) was observed. Furthermore, after the reduction process, the particle size of metallic Ni also increased upon increasing the Ni loading; however, the particle size of the reduced Ni was slightly lower than that of unreduced NiO.

Also, the N_2-sorption isotherms of the Ni(x)/Al_2O_3 catalysts indicated typical type IV isotherms due to their mesoporous struc-

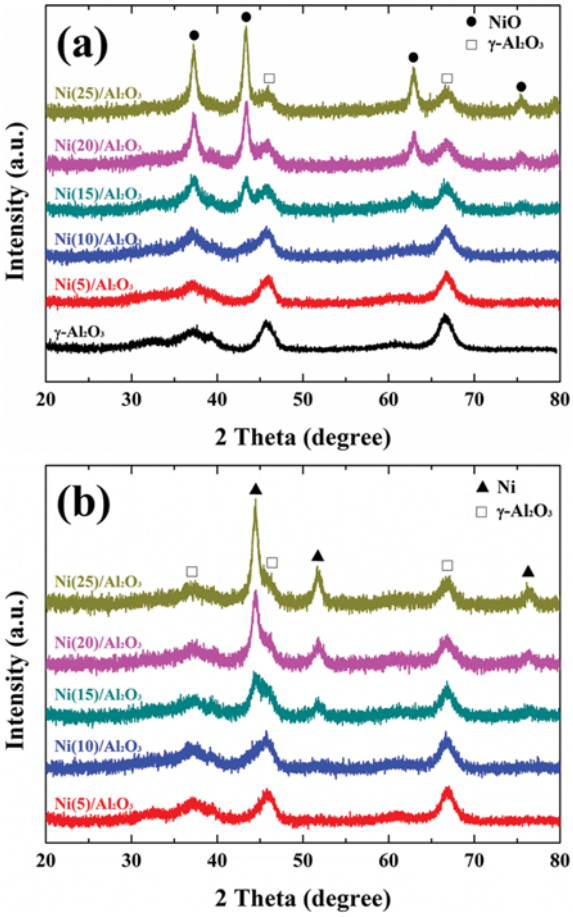

Fig. 2. XRD patterns of the Ni(x)/Al_2O_3 catalysts (a) calcined at 500 °C for 2 h and (b) reduced at 600 °C for 3 h.

Table 1. Textural and crystalline properties of the Ni(x)/Al_2O_3 catalysts. The particle sizes were calculated from the XRD patterns, while the specific surface areas (S_{BET}), total pore volumes (V_P), and average pore diameters (D_P) were determined by N_2-sorption isotherms

x in Ni(x)/Al_2O_3	XRD Particle size (nm)		N_2-sorption		
	NiO[a] (2θ=43.4°)	Ni[a] (2θ=44.5°)	S_{BET} (m^2/g)	V_P (cm^3/g)	D_P (nm)
0	-	-	194	0.699	14.5
5	-	-	163	0.593	14.3
10	-	-	157	0.561	13.8
15	14.2	11.4	144	0.487	13.3
20	14.8	12.1	136	0.463	13.2
25	17.6	14.6	125	0.375	12.0

[a]NiO and Ni particle sizes were calculated using the Scherrer equation with XRD patterns of the calcined and reduced catalysts, respectively

Table 2. Dispersions, particle sizes, and surface areas of the nickel species measured by H_2 chemisorption, and reduction degree obtained using an O_2 titration method

x in $Ni(x)/Al_2O_3$	O_2 titration	H_2 chemisorption					
	Reduction degree (%)	Uncorrected		Corrected		Metallic surface area	
		Dispersion (%)	Particle size (nm)	Dispersion (%)[a]	Particle size (nm)[b]	m^2/g_{Ni}	$m^2/g_{cat.}$
5	36.0	3.9	25.4	11.1	9.1	21.1	1.1
10	48.8	5.8	16.8	12.0	8.1	31.4	3.1
15	49.1	4.0	25.2	8.2	12.4	21.0	3.2
20	50.3	3.5	28.6	7.0	14.4	19.5	3.9
25	51.4	3.4	29.8	6.6	15.3	19.0	4.8

[a]Corrected dispersion=surface Ni^0 atom/total reduced Ni^0 atom×100=surface Ni^0 atom/(total Ni atom×reduced fraction)×100
[b]Corrected Ni diameter=uncorrected Ni diameter×reduced Ni fraction

tures (isotherm data not shown). Based on the obtained results, the specific surface areas, total pore volumes, and average pore sizes of the calcined $Ni(x)/Al_2O_3$ catalysts are summarized in Table 1. As indicated, upon increasing the Ni loading, the specific surface area decreased gradually from 194 to 125 m^2/g, accompanied by a decrease in the total pore volume. These observations are attributed to a partial blockage of the pores in the γ-Al_2O_3 support by the impregnated Ni species.

As previously reported, valuable and quantitative information regarding the impregnated Ni species can be collected from H_2 chemisorption data, such as the number of exposed metal sites and the particle size [13,19]. As shown in Table 2, the H_2 chemisorption results (e.g., the dispersion and particle size of the Ni species) were corrected by the reduction degree measured from the O_2 titration method. Although the areas of fully exposed metallic sites (metallic surface area, m^2/g_{cat}) were higher at higher Ni loadings, the corrected metal dispersion showed a volcano-shaped curve as a function of Ni loading, where the highest value (i.e., 12.0%) was obtained for the $Ni(10)/Al_2O_3$ catalyst. Indeed, this result is in good agreement with the XRD results. Furthermore, as the Ni content was increased, the metal dispersion gradually decreased above a Ni loading of 10 wt%, while the particle size increased. As a result, for the $Ni(25)/Al_2O_3$ catalyst, the metal dispersion decreased to 6.6%, and the particle size of the Ni species increased to 15.3 nm.

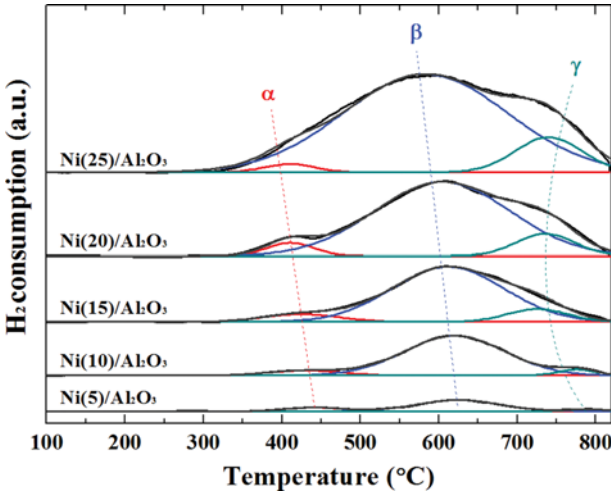

Fig. 3. H_2-TPR profiles of the $Ni(x)/Al_2O_3$ catalysts. All samples were calcined at 500 °C for 2 h prior to H_2-TPR measurements.

H_2-TPR experiments were performed to investigate both the reducibility of the nickel species and the metal-support interactions [23-25]. The H_2-TPR profiles of the calcined catalysts are shown in Fig. 3, and the evolved peak temperatures and relative proportions of the peak areas are listed in Table 3. Three different stages of reduction can be observed for all samples, i.e., at 400-450 °C (α peak), 550-700 °C (β peak), and 650-800 °C (γ peak) [13,19,23-26]. More specifically, the α peak was ascribed to the reduction of NiO species that interacted weakly with the Al_2O_3 support, the β peak was mainly derived from strong interactions between the NiO species and the support, and the γ peak was assigned to the reduction of nickel aluminate. The complete reduction of Ni species is particularly difficult due to the high reduction temperature of nickel aluminate. In this case, the peak intensities (i.e., areas) of the α and β peaks increased continuously as a function of Ni loading, and the evolved peak temperatures shifted towards lower temperatures, indicating that higher metal loadings induced the formation of bulk NiO species with weak metal-support interactions, which exhibited enhanced reducibility. This result is in good agreement with the results of O_2 titration analysis (Table 2), in which the reduction degree of the calcined catalysts increased from 36.0 to 51.4% as the Ni loading was increased from 5 to 25 wt%. In addition, the reduction temperature associated with the γ peak decreased with increasing Ni loading up to 15 wt%, although it increased once again above this point. Although the peak temperature of the γ peak varied with Ni loading, the total reduc-

Table 3. Evolved peak temperatures and relative proportions of peak areas obtained from the H_2-TPR profiles of the $Ni(x)/Al_2O_3$ catalysts. All samples were calcined at 500 °C for 2 h prior to the H_2-TPR measurements

x in $Ni(x)/Al_2O_3$	Peak temperature (°C) (relative proportion, %)		
	α	β	γ
5	442 (17)	625 (77)	790 (6)
10	430 (8)	620 (87)	776 (5)
15	425 (7)	612 (83)	726 (10)
20	411 (5)	605 (84)	736 (11)
25	410 (3)	583 (84)	740 (13)

tion of nickel aluminate to metallic Ni is not facile in the experimental conditions employed herein (i.e., reduction at 600 °C) due to requirement for a high reduction temperature for this process (i.e., >700 °C) [13,19,23-26].

As previously mentioned, a metallic function is required for the reductive amination reaction to take place. Therefore, shifts in the α and β peaks towards lower temperatures in addition to increases in the α and β peak intensities as a function of Ni loading will have a positive effect on catalytic activity for the reductive amination process. However, we expect that an optimal Ni composition must exist for the Ni(x)/Al_2O_3 catalysts, as an increase in the γ peak intensity imparts a negative effect on the catalytic process (see the following section for further details).

2. Reductive Amination of Ethanol over the Prepared Ni(x)/Al_2O_3 Catalysts

We then investigated the influence of Ni loading on the conversion and selectivity in the reductive amination of EtOH at 190 °C, with a WHSV of 0.9 h^{-1}, and an EtOH/NH_3/H_2 molar ratio of 1/3/6. Fig. 4 shows the conversion of EtOH and the selectivities to the different products as a function of Ni loading, where all data was obtained following 3 h on stream. The initial conversion of EtOH slightly decreased, but it was almost constant after 3 h on stream for 13 h (not shown here). As mentioned during discussion of the H_2-TPR results, the conversion of EtOH exhibits a volcano-shaped curve as a function of Ni loading, with a maximum value of 76.5% over the Ni(10)/Al_2O_3 catalyst. As such, the EtOH conversion of the different Ni(x)/Al_2O_3 catalysts decreased in the following order: x=10>15>20>25>5. In addition, among the various products produced through the reductive amination reaction, MEA and DEA were the main products, although TEA, acetonitrile (ACN), and ethylene were also detected. In all samples, the sum of the selectivities to MEA, DEA, and TEA exceeded 85%, indicating that the majority of EtOH molecules were converted to EAs. These results also indicate that the amination reaction was more favorable than dehydration to ethylene under the given reaction conditions. Unlike the EtOH conversion trend, the obtained selectivities did not differ significantly upon variation in the Ni loading. However, the MEA selectivity was slightly higher for the Ni(5)/Al_2O_3 catalyst, while the selectivity to DEA was rather higher for the Ni(10)/Al_2O_3 catalyst. This was likely due to the relatively high catalytic activity of the Ni(10)/Al_2O_3 catalyst, as this system resulted in both the highest EtOH conversion and the highest selectivity to DEA [1,2].

As a metallic functionality is required to participate in the hydrogenation/dehydrogenation steps in the reductive amination process, the area of exposed metal sites, resulting from metal dispersion and the metallic surface area, was found to be closely related to catalytic performance [1,9,13,14]. As outlined in Table 2, the area of totally exposed metal sites (m^2/g_{cat}) increased with increasing Ni loading, while the metallic surface area per unit mass of Ni (m^2/g_{Ni}) exhibited a volcano-shaped curve, which correlated well with the EtOH conversion discussed above. These observations indicate that not all metallic sites participated in the reaction, but rather that they reacted selectively. Indeed, similar results can be found in the literature [13,14]. Cho et al. [13] studied the reductive amination of *iso*-propanol to monoisopropylamine with variation in Ni loading on a γ-Al_2O_3 support. They claimed that the metallic surface area (m^2/g_{cat}) correlated with the EtOH conversion, but that it was not matched at a high Ni loading (27 wt%).Chary et al. [14] performed the reductive amination of cyclohexanol over Cu/ZrO_2 catalysts, and the obtained conversion correlated well with the metallic surface area per unit mass of Cu (m^2/g_{Cu}). It is therefore likely that the reaction is occurring at the metal-support interface, as the acidic function of the support can promote the reductive amination process [1,14,19].

Amongst the examined catalysts, the Ni(10)/Al_2O_3 catalyst exhibited a superior catalytic performance (Fig. 4) in the reductive amination of EtOH, likely due to this catalyst exhibiting the highest metal dispersion and metallic surface area (m^2/g_{Ni}, see Table 2). In addition, although the Ni(5)/Al_2O_3 and Ni(15)/Al_2O_3 catalysts have similar metallic surface areas (i.e., ~21 m^2/g_{Ni}), the Ni(15)/Al_2O_3

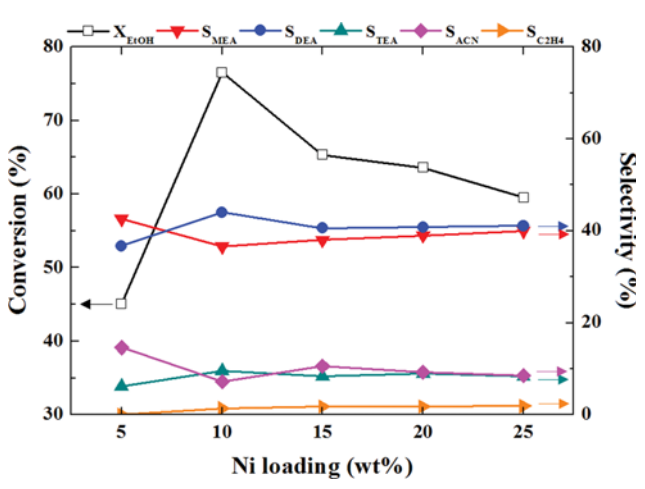

Fig. 4. Conversion of ethanol and selectivities to ethylamines, acetonitrile, and ethylene over Ni(x)/Al_2O_3 catalysts.. Reaction conditions: T=190 °C, WHSV=0.9 h^{-1}, and EtOH/NH_3/H_2 molar ratio=1/3/6.

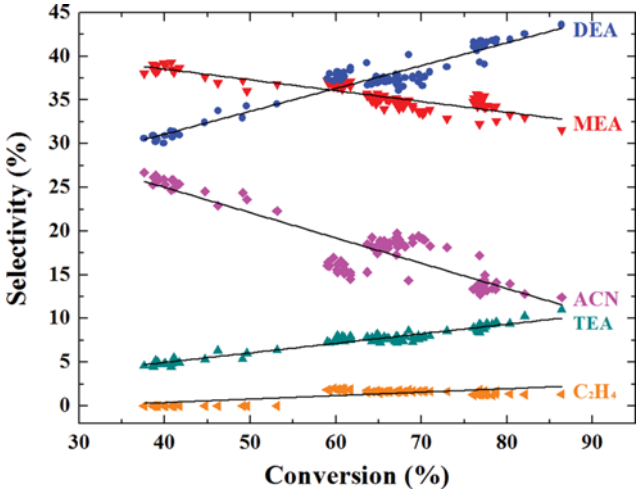

Fig. 5. Selectivity distributions of the ethylamines, acetonitrile, and ethylene as a function of ethanol conversion for the Ni(x)/Al_2O_3 catalysts. Reaction conditions: T=190 °C, WHSV=0.9 h^{-1}, and EtOH/NH_3/H_2 molar ratio=1/3/6.

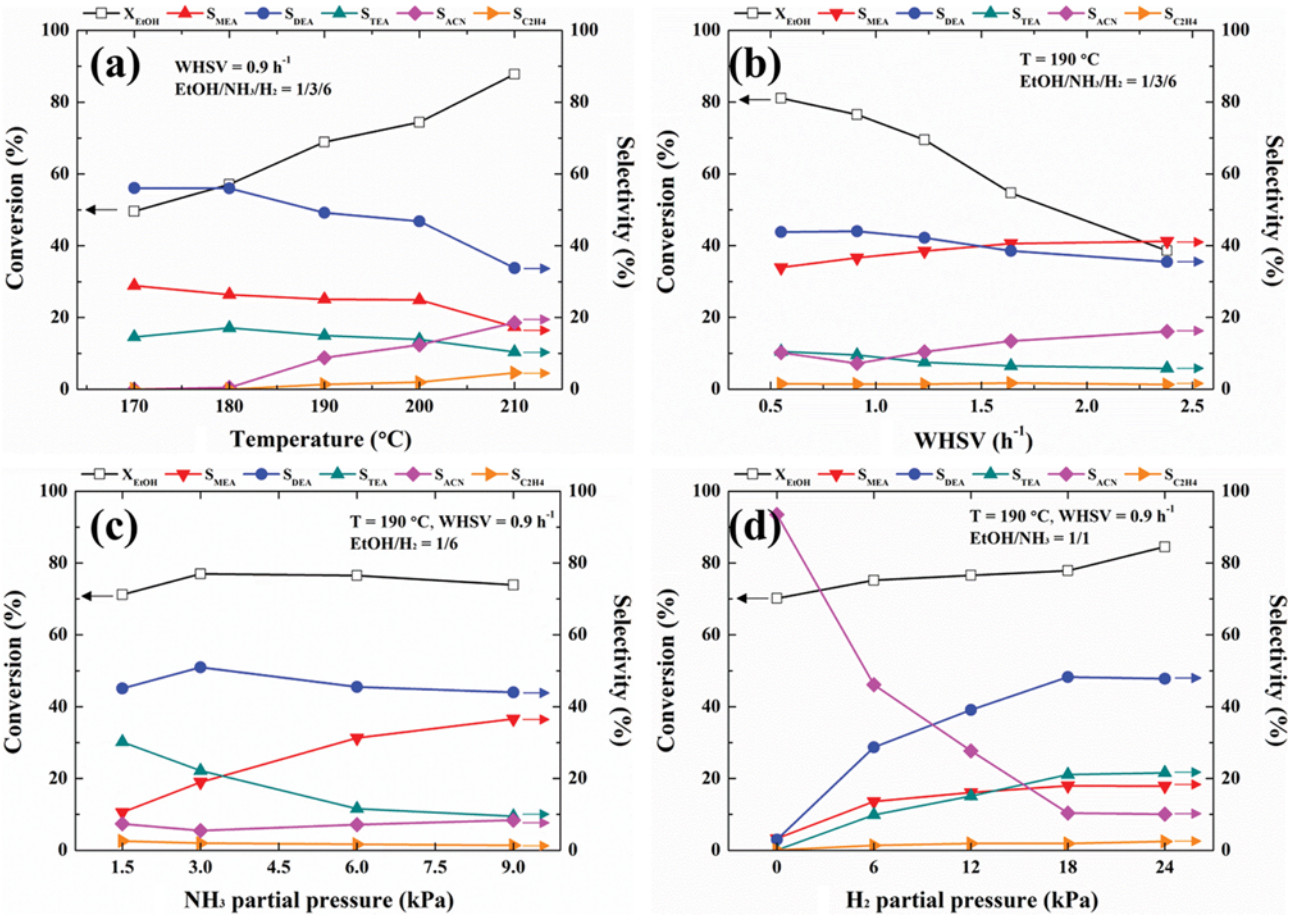

Fig. 6. Effects of varying the reaction parameters on the reductive amination process over the $Ni(10)/Al_2O_3$ catalyst: (a) Reaction temperature, (b) WHSV, (c) NH_3 partial pressure, and (d) H_2 partial pressure.

catalyst exhibited higher EtOH conversion than the $Ni(5)/Al_2O_3$ catalyst, which could potentially be attributed to the metal-support interactions discussed in the H_2-TPR results (Fig. 3 and Table 3). More specifically, H_2-TPR measurements indicated that the $Ni(15)/Al_2O_3$ catalyst has a lower reduction peak temperature than the $Ni(5)/Al_2O_3$ catalyst, indicating that the metal-support interactions were weaker. As such, the active sites present in the $Ni(15)/Al_2O_3$ catalyst can more readily participate in the amination reaction.

Fig. 5 shows the selectivity distributions of the EAs, ACN, and ethylene as a function of the EtOH conversion. To obtain this selectivity distribution, reductive amination was performed using the $Ni(x)/Al_2O_3$ catalysts under identical reaction conditions over 13 h (i.e., T=190 °C, WHSV=0.9 h^{-1}, and $EtOH/NH_3/H_2$ molar ratio=1/3/6). As the EtOH conversion increased, the MEA selectivity decreased, while the selectivity towards DEA and TEA gradually increased. This result suggests that DEA and TEA were produced from MEA as a consecutive reaction (indicated in Fig. 1, and so the synthesis of DEA and TEA was more favorable at higher EtOH conversion. On the other hand, the selectivity towards ACN, which was generated from the dehydrogenation of either the imine intermediate or MEA, decreased upon increasing the EtOH conversion. Furthermore, the ethylene selectivity remained relatively constant at ~1.5% for all conversion values, indicating that EtOH dehydrogenation occurs more selectively than dehydration.

To achieve the best catalytic performance, the influence of the reaction parameters, including the reaction temperature, WHSV, and NH_3 and H_2 partial pressures, was investigated for the reductive amination of EtOH over the $Ni(10)/Al_2O_3$ catalyst. As shown in Fig. 6(a), upon variation of the reaction temperature between 170 and 210 °C (WHSV=0.9 h^{-1}, $EtOH/NH_3/H_2$ molar ratio=1/3/6), an increase in temperature resulted in a continuous increase in EtOH conversion. In addition, the selectivities towards the different EAs rapidly decreased from 99.6% at 170 °C to 61.6% at 210 °C, which was compensated by an increase in ACN formation. This result implied that although ACN could be produced from the imine intermediate, it was mainly produced from MEA under the reaction conditions employed herein. Indeed, ACN formation from the dehydrogenation of MEA was promoted at higher temperatures, thus competing with the formation of DEA from MEA.

The effect of the WHSV between 0.55 and 2.38 h^{-1} was then examined at 190 °C with a $EtOH/NH_3/H_2$ molar ratio of 1/3/6, as shown in Fig. 6(b). As an increase in WHSV results in a reduced contact time between the reactant and the catalyst [2], a decrease in EtOH conversion was observed from 81.1 to 38.6% upon increasing the WHSV. Furthermore, the reduction in contact time

upon increasing the WHSV also resulted in increased selectivity to both MEA and ACN, likely due to the formation of DEA and TEA being hindered by decreasing the contact time.

Fig. 6(c) shows the effect of varying the NH_3 partial pressure (1.5-9 kPa) on the reductive amination of EtOH when the experiments were carried out at 190 °C with a WHSV of 0.9 h^{-1} and an EtOH/H_2 molar ratio of 1/6. As indicated, the EtOH conversion reached a maximum of 77.0% at an NH_3 partial pressure of 3 kPa, and it decreased at higher NH_3 partial pressures. This may be due to the formation of nickel nitride ($3Ni+NH_3 \rightarrow Ni_3N+3/2H_2$) at high NH_3 partial pressures [13,20,21]. In addition, MEA formation became more favorable as the NH_3 partial pressure was increased, while the selectivity towards DEA and TEA decreased [2]. This could be accounted for by competitive adsorption, where an excess of NH_3 inhibits the formation of DEA and TEA by interfering with the adsorption of EtOH [2]. We therefore considered an NH_3 partial pressure of 3 kPa to be optimal for the reductive amination of EtOH.

The effect of H_2 partial pressure was also investigated at 190 °C with a WHSV of 0.9 h^{-1} and an EtOH/NH_3 molar ratio of 1/1, as outlined in Fig. 6(d). In the absence of H_2, the EtOH conversion gradually decreased as the reaction proceeded due to the formation of nickel nitride [13,20,21] (data not shown, but will be discussed later part), resulting in ACN being the main product. However, upon increasing the H_2 partial pressure from 0 to 24 kPa, the ACN selectivity decreased to 10.1%, accompanied by an increase in EtOH conversion [2].

Thus, as demonstrated in the results shown in Fig. 6, the partial pressures of NH_3 and H_2 have a significant influence on the EtOH conversion and the selectivity towards the different EAs over the Ni(10)/Al_2O_3 catalyst. To further understand the effect of the reactants on the reductive amination of EtOH, on/off experiments of NH_3 and H_2 were carried out as shown in Fig. 7. For the initial stage, the reaction conditions were as follows: T=190 °C, WHSV=0.9 h^{-1}, and EtOH/NH_3/H_2 molar ratio=1/3/6. In addition, N_2 was used to complement the total flow (50 cm^3/min) in the absence of NH_3 and H_2. During the initial 10 h under these conditions, slight deactivation of the catalyst was observed, resulting in a decrease in the EtOH conversion from 79.9 to 76.1%. After the NH_3 stream was turned off, the EtOH conversion decreased sharply, and no nitrogen-containing compounds were detected in the products. Indeed, dehydration/dehydrogenation products dominated, including ethylene, ethane, and acetaldehyde. When the reactant composition was switched back to the initial conditions, the EtOH conversion and selectivity recovered to their initial values. Subsequent removal of H_2 from the reactant stream resulted in the formation of mainly ACN through dehydrogenation of the imine intermediate and MEA. This result therefore confirmed the observation described above for Fig. 6(d). Again, when the reactant composition was returned to its initial conditions, the EtOH conversion and product selectivity fully recovered to their initial values. These results therefore indicate that although a slight deactivation of the catalyst was observed during the initial reaction period, the reductive amination proceeded stably under the reaction conditions employed herein. In addition, the influence of NH_3 and H_2 partial pressures on EtOH conversion and product selectivity were clearly confirmed, and these factors are key parameters for controlling the product distributions of the EAs and ACN in the reductive amination of EtOH.

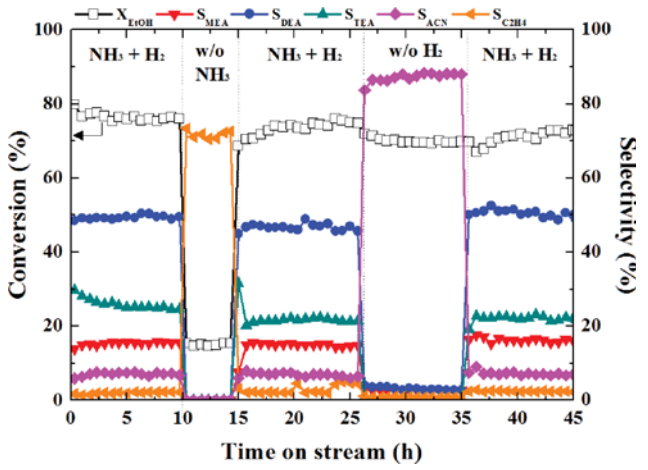

Fig. 7. Conversions and selectivities as a function of time on stream in the presence and absence of NH_3 and H_2 over the Ni(10)/Al_2O_3 catalyst at T=190 °C, where WHSV=0.9 h^{-1} and the EtOH/NH_3/H_2 molar ratio=1/1/6. In the absence of NH_3 or H_2, the corresponding amount of each reactant stream was compensated by a flow of N_2.

3. Long-term Stability Test

The stability of a catalyst during its intended reaction period is an important parameter for determining catalyst performance and its suitability to industrial applications. We therefore did a long-term stability test for the reductive amination of EtOH over the Ni(10)/Al_2O_3 catalyst for 90 h (reaction conditions: T=190 °C, WHSV=0.9 h^{-1}, and EtOH/NH_3/H_2 molar ratio=1/1/6). As shown in Fig. 8, the EtOH conversion decreased from 81.9 to 72.1% during the initial 10 h prior to reaching a relatively constant value of ~69% after 15 h. In addition, the selectivity to the different EAs was also maintained at >80% over 90 h, thereby indicating that the Ni(10)/Al_2O_3 catalyst is a promising candidate for the practical

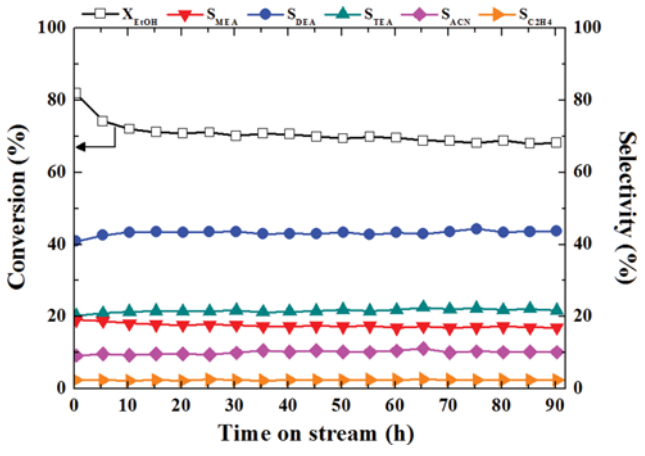

Fig. 8. Long-term stability of the Ni(10)/Al_2O_3 catalyst in the reductive amination of ethanol. Reaction conditions: T=190 °C, WHSV=0.9 h^{-1}, and EtOH/NH_3/H_2 molar ratio=1/1/6.

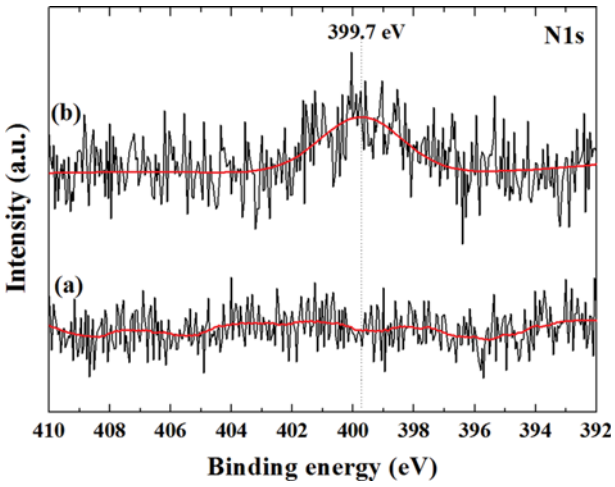

Fig. 9. N 1s spectra obtained from XPS measurements of the Ni(10)/Al_2O_3 catalyst at different reaction stages: (a) After reduction at 600 °C for 3 h (before reaction), and (b) after reaction for 90 h on stream.

reductive amination of EtOH, due to its high catalytic activity and stability.

As one can see in Fig. 8, the conversion of EtOH was mainly reduced in the initial stage, and then stabilized. To determine why such catalyst deactivation occurred in the initial stages of the reaction, XPS analysis of the $Ni(10)/Al_2O_3$ catalyst was conducted, and the N 1s XPS spectra of the $Ni(10)/Al_2O_3$ catalyst both before (after reduction at 600 °C for 3 h) and after the 90 h reaction are shown in Fig. 9. Although oxidation of the reduced Ni species during the reaction could potentially account for the observed deactivation, the formation of metal nitrides is likely to be the main cause. Indeed, the formation of this species was confirmed by the absence of an N 1s peak in the XPS spectrum before the reaction, and the presence of a peak at 399.7 eV after the reaction, which corresponded to nickel nitride [27,28]. These results indicate that nickel nitride was formed by a reaction between the metallic Ni species and the introduced NH_3 (or the produced EAs compounds) during the reductive amination of EtOH as shown in the below equations.

$$NH_3+3Me\leftrightarrow Me_3N+3/2H_2$$
$$2(C_2H_5\text{-}NH_2)+3Me\leftrightarrow Me_3N+3/2H_2+(C_2H_5)_2NH$$
$$3(C_2H_5\text{-}NH_2)+6Me\leftrightarrow 2Me_3N+3H_2+(C_2H_5)_3N$$

where Me is metal sites on catalyst surface. Therefore, we can expect that nickel nitride was formed mainly in the initial period of the reaction, thus allowing the catalytic performance to be stably maintained for 90 h after this initial period under the optimized experimental conditions described herein.

CONCLUSIONS

The reductive amination of EtOH was examined over $Ni(x)/Al_2O_3$ (x=wt%) catalysts with different nickel loadings in the range of 5-25 wt%, and the $Ni(10)/Al_2O_3$ catalyst exhibited the best catalytic performance. Interestingly, this catalyst was found to exhibit the smallest Ni particle size and the highest metal dispersion. In terms of catalyst performance, over long-term stability tests (i.e., over 90 h), the EtOH conversion decreased slightly during the initial 10 h of the reaction due to formation of the metal nitride, but a relatively stable conversion was maintained after this period. In addition, the partial pressures of NH_3 and H_2 influenced on EtOH conversion and product selectivities. An excess of NH_3 in the reactant stream increased the selectivity towards monoethylamine, while an increase in the H_2 partial pressure increased overall selectivities to the different ethylamine products. In addition, the conversion of EtOH also varied with NH_3 and H_2 partial pressures. These results therefore indicate that the EtOH conversion and product selectivities can be tuned by controlling the reaction parameters outlined above.

ACKNOWLEDGEMENT

This research was supported by Basic Science Research Program through the National Research Foundation of Korea (NRF) funded by the Ministry of Science, ICT & Future Planning (2017R1A2B3011316).

REFERENCES

1. G. S. Sewell, C. T. O'Connor and E. van Steen, *J. Catal.*, **167**, 513 (1997).
2. G. Sewell, C. O'Connor and E. Van Steen, *Appl. Catal. A: Gen.*, **125**, 99 (1995).
3. K. Hayes, *Appl. Catal. A: Gen.*, **221**, 187 (2001).
4. R. Reguillo, M. Grellier, N. Vautravers, L. Vendier and S. Sabo-Etienne, *J. Am. Chem. Soc.*, **132**, 7854 (2010).
5. S. Das, S. Zhou, D. Addis, S. Enthaler, K. Junge and M. Beller, *Top. Catal.*, **53**, 979 (2010).
6. R. P. Tripathi, S. S. Verma, J. Pandey and V. K. Tiwari, *Curr. Org. Chem.*, **12**, 1093 (2008).
7. J. Seayad, A. Tillack, C. G. Hartung and M. Beller, *Adv. Syn. Catal.*, **344**, 795 (2002).
8. S. Bähn, S. Imm, L. Neubert, M. Zhang, H. Neumann and M. Beller, *ChemCatChem*, **3**, 1853 (2011).
9. J. H. Cho, J. H. Park, T.-S. Chang, G. Seo and C.-H. Shin, *Appl. Catal. A: Gen.*, **417-418**, 313 (2012).
10. S. Gomez, J. A. Peters and T. Maschmeyer, *Adv. Syn. Catal.*, **344**, 1037 (2002).
11. V. Zamlynny, L. Kubelková, E. Babůrek, K. Jirátová and J. Nováková, *Appl. Catal. A: Gen.*, **169**, 119 (1998).
12. Y. Zhang, Y. Zhang, C. Feng, C. Qiu, Y. Wen and J. Zhao, *Catal. Commun.*, **10**, 1454 (2009).
13. J. H. Cho, J.-H. Park, T.-S. Chang, J.-E. Kim and C.-H. Shin, *Catal. Lett.*, **143**, 1319 (2013).
14. K. V. Chary, K. K. Seela, D. Naresh and P. Ramakanth, *Catal. Commun.*, **9**, 75 (2008).
15. J. Bódis, L. Lefferts, T. Müller, R. Pestman and J. Lercher, *Catal. Lett.*, **104**, 23 (2005).
16. T. Ikenaga, K. Matsushita, J. Shinozawa, S. Yada and Y. Takagi, *Tetrahedron*, **61**, 2105 (2005).
17. M. Ousmane, G. Perrussel, Z. Yan, J.-M. Clacens, F. De Campo

and M. Pera-Titus, *J. Catal.*, **309**, 439 (2014).
18. M. E. Domine, M. C. Hernández-Soto, M. T. Navarro and Y. Pérez, *Catal. Today*, **172**, 13 (2011).
19. J. H. Cho, S. H. An, T.-S. Chang and C.-H. Shin, *Catal. Lett.*, **146**, 811 (2016).
20. A. Baiker, W. Caprez and W. L. Holstein, *Ind. Eng. Chem. Prod. RD.*, **22**, 217 (1983).
21. A. Baiker, D. Monti and Y. S. Fan, *J. Catal.*, **88**, 81 (1984).
22. J. W. Bae, S.-M. Kim, S.-H., Kang, K. V. Chary, Y.-J. Lee, H.-J. Kim and K.-W. Jun, *J. Mol. Catal. A: Chem.*, **311**, 7 (2009).
23. R. Yang, X. Li, J. Wu, X. Zhang, Z. Zhang, Y. Cheng and J. Guo, *Appl. Catal. A: Gen.*, **368**, 105 (2009).
24. R. Yang, J. Wu, X. Li, X. Zhang, Z. Zhang and J. Guo, *Appl. Catal. A: Gen.*, **383**, 112 (2010).
25. M. Zangouei, A. Z. Moghaddam and M. Arasteh, *Chem. Eng. Res. Bull.*, **14**, 97 (2010).
26. C. Li and Y.-W. Chen, *Thermochim. Acta*, **256**, 457 (1995).
27. I. K. Milad, K. J. Smith, P. C. Wong and K. A. Mitchell, *Catal. Lett.*, **52**, 113 (1998).
28. I. Milošev, H.-H. Strehblow and B. Navinšek, *Thin Solid Films*, **303**, 246 (1997).